



RESEARCH ARTICLE

MALDI-MS/MS with Traveling Wave Ion Mobility for the Structural Analysis of *N*-Linked Glycans

David J. Harvey,^{1,2} Charlotte A. Scarff,^{2,3} Max Crispin,¹ Christopher N. Scanlan,¹
Camille Bonomelli,¹ James H. Scrivens²

¹Oxford Glycobiology Institute, Department of Biochemistry, University of Oxford, South Parks Road, Oxford, OX1 3QU, UK

²Department of Biological Sciences, University of Warwick, Coventry, CV4 7AL, UK

³Astbury Centre for Structural Molecular Biology, University of Leeds, Leeds, LS2 9JT, UK

Abstract

The preference for singly charged ion formation by MALDI makes it a better choice than electrospray ionization for profiling mixtures of *N*-glycans. For structural analysis, fragmentation of negative ions often yields more informative spectra than fragmentation of positive ones but such ions are more difficult to produce from neutral glycans under MALDI conditions. This work investigates conditions for the formation of both positive and negative ions by MALDI from *N*-linked glycans released from glycoproteins and their subsequent MS/MS and ion mobility behaviour. 2,4,6-Trihydroxyacetophenone (THAP) doped with ammonium nitrate was found to give optimal ion yields in negative ion mode. Ammonium chloride or phosphate also yielded prominent adducts but anionic carbohydrates such as sulfated *N*-glycans tended to ionize preferentially. Carbohydrates adducted with all three adducts (phosphate, chloride, and nitrate) produced good negative ion CID spectra but those adducted with iodide and sulfate did not yield fragment ions although they gave stronger signals. Fragmentation paralleled that seen following electrospray ionization providing superior spectra than could be obtained by PSD on MALDI-TOF instruments or with ion traps. In addition, ion mobility drift times of the adducted glycans and the ability of this technique to separate isomers also mirrored those obtained following ESI sample introduction. Ion mobility also allowed profiles to be obtained from samples whose MALDI spectra showed no evidence of such ions allowing the technique to be used in conditions where sample amounts were limiting. The method was applied to *N*-glycans released from the recombinant human immunodeficiency virus glycoprotein, gp120.

Key words: T-wave ion mobility, *N*-linked carbohydrates, Isomers, Negative ion MALDI, HIV

Abbreviations: ATD Arrival time distribution; ATT 6-azo-2-thiothymine; CID collision-induced dissociation; DHAP 2,5-dihydroxybenzoic acid; DHB 2,5-dihydroxybenzoic acid; ESI electrospray ionization; FAB fast atom bombardment; Fuc fucose; Gal galactose; GlcNAc *N*-acetylglucosamine; HABA 2-(4'-hydroxyphenylazo)benzoic acid; HEK human embryonic kidney; HIV human immunodeficiency virus; HPLC high performance liquid chromatography; MALDI matrix-assisted laser desorption/ionization; Man mannose; PNGase peptide *N*-glycosidase; PSD post-source decay; Q quadrupole; MS mass spectrometry; THAP 2,4,6-trihydroxyacetophenone; TOF time-of-flight; TWIMS travelling-wave ion mobility mass spectrometry

Electronic supplementary material The online version of this article (doi:10.1007/s13361-012-0425-8) contains supplementary material, which is available to authorized users.

Correspondence to: David J. Harvey; e-mail: david.harvey@bioch.ox.ac.uk

Published online: 20 September 2012

Introduction

Post-translational modifications can significantly diversify the biology of proteins. One of the most abundant

Received: 2 March 2012
Revised: 24 April 2012
Accepted: 29 May 2012

modifications of secreted and cell-surface proteins is *N*-linked glycosylation. *N*-glycans are branched carbohydrates attached to asparagine in glycoproteins where the asparagine is in an Asn-Xxx-Ser(Thr) sequence where Xxx is any amino acid except proline [1]. Their analysis has received much attention over the past three decades and involves techniques such as HPLC, exoglycosidase sequencing, and mass spectrometry [2–13]. The introduction of fast-atom bombardment (FAB) mass spectrometry in the 1980s catalysed much work on the positive ion mass spectrometry of permethylated glycans [14–18] but FAB has now largely been replaced by ionization using matrix-assisted laser desorption/ionization (MALDI) [3, 19] and electrospray ionization (ESI) mass spectrometry [20], which enable both derivatized and underivatized glycans to be examined. Nevertheless, positive ionization remains the most popular mode, and permethylation is still widely used for purposes such as increasing ion yields and providing linkage information by fragmentation [21]. Under positive ion conditions, carbohydrates undergo fragmentation mainly by glycosidic (between the sugar rings) bond cleavage with formation of the more informative cross-ring fragments being a relatively minor process unless high collision energies are employed [22–24]. A problem with positive ion fragmentation is that many of the glycosidic fragments arise from multiple pathways [25] meaning that for an unknown compound, it is difficult to extract the necessary structural information. Permethylation or MSⁿ experiments [26–28] help in this context but some structural features still remain difficult to determine.

Negative ion fragmentation, on the other hand, produces spectra that are dominated by cross-ring cleavage fragments that arise by specific pathways and provide a wealth of structural information [29–32]. Most of the work in this area has been performed with electrospray ionization which has the disadvantages of multiple charging, discrimination against the larger glycans and formation of in-source fragments leading to rather complex spectra. MALDI is a more satisfactory technique for obtaining glycan profiles of neutral carbohydrates although sialylated compounds tend to eliminate sialic acids under MALDI conditions unless derivatized by, for example, permethylation, methyl ester [33, 34] or amide [35] formation. Neutral glycans, however, do not easily form ions by MALDI in negative ion mode with the normal matrices such as 2,5-dihydroxybenzoic acid (DHB) but can be induced to do so by use of matrices such as *nor*-harmane [36] or by adding suitable anions to the matrix [37–43]. The latter technique has the advantage of stabilizing the ions as adducts because the largely $[M - H]^-$ ions that are produced by the other methods are relatively unstable and more difficult to transfer to collision cells for subsequent fragmentation.

We have recently investigated conditions for obtaining negative ion spectra from neutral *N*-glycans for examination by MALDI-TOF MS by adduct formation [44] and have found that addition of ammonium nitrate to 2,4,6-trihydroxyacetophenone (THAP) gives good results. Adduction with chloride, as used by others [37–40, 45–49], has the disadvantage of a split signal due to the chlorine isotopes. Phosphate, which has proven to be most

appropriate under electrospray conditions [32], did not form very abundant ions under MALDI conditions. However, as pointed out previously, the use of chloride, phosphate or nitrate as the adduct makes little difference to the fragmentation pattern because the initial event following collisional activation is proton abstraction by the adduct to give a $[M - H]^-$ ion [30].

With the advent of MALDI ion sources fitted to Q-TOF instruments, collision-induced dissociation (CID) spectra can be obtained that do not suffer from the low resolution inherent to post-source decay (PSD) spectra or the low mass cut-off that is the consequence of data acquisition with ion traps. The addition of ion-mobility on instruments such as the Waters Synapt (Waters MS Technologies, Manchester, UK) adds another dimension to glycan analysis and, in this paper, we explore the use of this instrument for obtaining predominantly negative ion MS/MS spectra of *N*-glycans and for obtaining additional structural information by ion mobility.

Materials and Methods

Materials

N-linked glycans were released in a large-scale preparation with hydrazine [50, 51] from the well-characterized glycoproteins (Sigma Chemical Co. Ltd., Poole, Dorset, UK) ribonuclease B [52], porcine thyroglobulin [53, 54], chicken ovalbumin (found to contain small amounts of other ovo-glycoproteins) [55, 56], and bovine fetuin [57]. Neutral glycans were obtained from fetuin and thyroglobulin by heating the released glycans with 1 % acetic acid for 1 h at 70 °C. *N*-glycans from the glycoprotein gp120 were released with peptide *N*-glycosidase F (PNGase F) from within SDS-PAGE gels as described previously [58] and also directly from solution. The human immunodeficiency virus (HIV) glycoprotein gp120_{BaL} was expressed in human embryonic kidney (HEK) 293T cells as previously described [59]. Methanol was obtained from BDH Ltd. (Poole, UK) ammonium salts were from Sigma-Aldrich, (Poole, UK). Water was distilled before use. DHB was from Sigma-Aldrich and was recrystallized from water. Other MALDI matrices were also from Sigma-Aldrich and were used without further purification.

Mass Spectrometry

Ion mobility experiments were carried out with a Waters Synapt G2 travelling wave ion mobility mass spectrometer (TWIMS) [60] fitted with electrospray and MALDI ion sources. The MALDI source used a Nd/Yag laser (355 nm). The T-wave velocity and peak height voltages were 450 m/s and 40 V respectively. The T-wave mobility cell was operated at a pressure of 0.55 mbar and contained nitrogen. The instrument was externally calibrated with sodium iodide (positive ion), sialylated glycans from bovine fetuin (ESI, negative ion) or dextran (nitrate adduct, MALDI, negative ion). Fragmentation was performed after mobility separation in the transfer cell with argon. Data acquisition and

processing were carried out by use of the Waters Driftscope (ver. 2.1) software and MassLynx (ver. 4.1) (Waters Corporation, Manchester, UK).

ESI Data Acquisition

For ESI, samples were dissolved in water:methanol (1:1, vol:vol) containing a trace of sodium chloride for positive ion spectra or 1 mM ammonium phosphate or nitrate for acquisition in negative ion mode. Samples were infused into the ion source with Waters nanospray capillaries. The ESI capillary voltage was 1.2 kV, the cone voltage was 20–180 V and the ion source temperature was maintained at 120 °C.

MALDI Data Acquisition

For positive ion MALDI acquisition, 0.5 μ L of the samples, in water (about 1 μ g/mL) were deposited on the MALDI target together with 0.5 μ L of the MALDI matrix (10 mg of

DHB in 1 mL of 1:1, vol:vol water:methanol containing a trace of sodium chloride) and allowed to dry under ambient conditions. The sample spot was then recrystallized from ethanol. Negative ion MALDI sample preparation involved spotting an aqueous solution of the sample (0.5 μ L) onto the target followed by 0.5 μ L of an aqueous solution of ammonium fluoride, chloride, bromide, iodide, sulfate, phosphate or nitrate (1 M, the concentration that gave the best results in the MALDI-TOF study [44]) and 0.5 μ L of acetone solutions of THAP, 2,5-dihydroxyacetophenone (DHAP), *nor*-harmane, esculetin (6,7-dihydroxycoumarin), 2-(4'-hydroxyphenylazo)benzoic acid (HABA) or 6-azo-2-thiothymine (ATT) and again allowing them to dry under ambient conditions. Collision energies for the CID spectra were in the range 50–120 eV depending on the mass of the ion being fragmented.

Positive ion MALDI-TOF-MS spectra were also recorded with a Waters ToFSpec reflectron-TOF 2E mass spectrometer (nitrogen laser) for comparative purposes. The acceler-

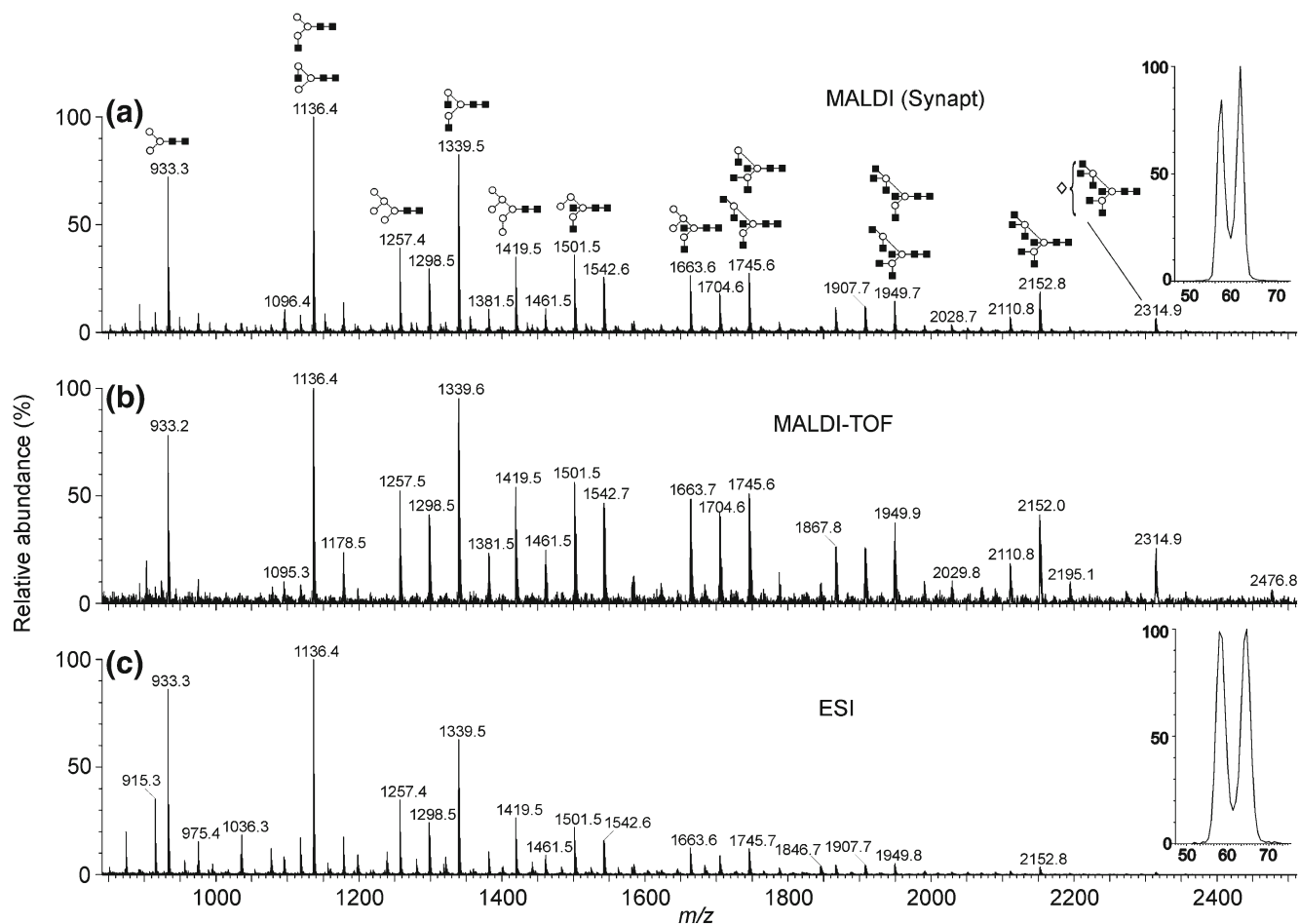


Figure 1. (a) Positive ion MALDI mass spectrum obtained with the Synapt instrument of *N*-glycans released from chicken ovalbumin ($[M+Na]^+$ ions). (b) MALDI-TOF spectrum of the same sample. (c) ESI spectrum (Synapt instrument) of the ovalbumin glycans. The insets show the TWIMS drift-time separations of isomers of the ion at m/z 1136 ($Man_3GlcNAc_3$). The first peak has the GlcNAc attached to the 3-antenna. Symbols for the glycan constituents and linkages between them in this and subsequent figures are: \blacksquare = GlcNAc, \circ = mannose, \diamond = galactose, \blacklozenge = fucose, \star = *N*-acetyl neuraminic acid (sialic acid). Solid connecting line = β -linkage, broken line = α -linkage. The angle of the lines shows the linkage position. For more information see [72]

ating voltage was 20 kV, the pulse voltage was 3200 V and the pulse delay was 500 ns. Sample processing was with MassLynx 4.1 as above.

Results and Discussion

Positive Ion

Neutral *N*-glycans released from ribonuclease B, porcine thyroglobulin, desialylated fetuin, and thyroglobulin, and from a mixture of ovalbumin and co-purified glycoproteins gave strong MALDI-TWIMS-MS spectra with a good signal:noise ratio and were very similar to those obtained from the same samples obtained with a MALDI-TOF instrument. Figure 1a shows the positive ion MALDI TWIMS-MS spectra from released ovalbumin glycans compared with the MALDI-TOF spectrum below (Figure 1b). These spectra were similar to each other but differed from the electrospray spectrum acquired with the Synapt instrument (Figure 1c), which showed a mass bias against the higher mass glycans. This phenomenon was at least partly attributable to differential double charging by the

larger compounds. Thus, MALDI would appear to offer distinct advantages over ESI on the Synapt instrument for this type of analysis. Sialylated glycans from bovine fetuin and thyroglobulin appeared to lose much less of their sialic acid than when examined with the MALDI-TOF system; spectra were compared with those of stable permethylated samples (spectra not shown). However, even if desialylation is a problem, previous work has shown that sialic acid loss can be prevented by derivatization of the carboxy group of the sialic acids by methyl ester [33, 34] or amide formation [35, 61] or by selective formation of lactones from $\alpha 2 \rightarrow 3$ -linked sialic acids [34] with retention of the free hydroxyl groups that are necessary for production of the informative negative ion CID spectra.

Earlier work [62] has demonstrated isomer separation by ion mobility of the two components of the ion at m/z 1136 from ovalbumin; this separation is shown as the inset to Figure 1c. After MALDI ionization, the same arrival time distribution and resolution for these components was seen in both positive ion (inset to Figure 1a) and negative ion modes showing that the type of ionization did not appear to affect the drift times or ability of the mobility cell to separate

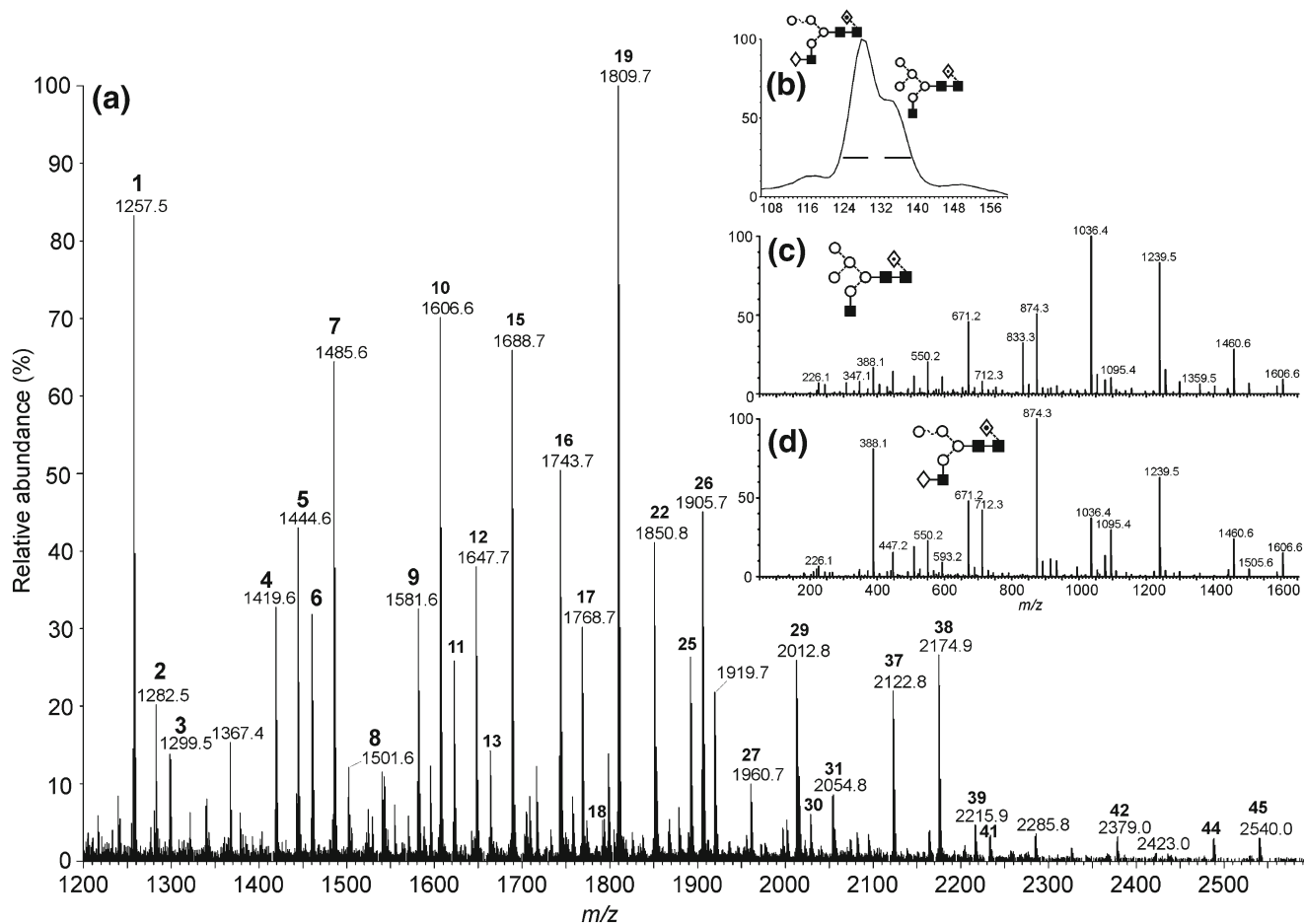


Figure 2. (a) Positive ion MALDI spectra of gp120 glycans released with PNGase F and ionized by MALDI from DHB. Peak identification is in Table 1 (columns 2 and 3). (b) Ion mobility separation of the two glycans of composition $\text{Hex}_5\text{GlcNAc}_3\text{Fuc}_1$ (m/z 1606 (10)). (c) CID spectra of the first region of the ATD peak shown by the horizontal line in (b), (d) CID spectrum of the second region

isomers. Neither did the type of ionization appear to affect the CID fragmentation acquired in the transfer cell (after mobility separation); spectra acquired in each case were virtually identical. Thus, in positive ion mode, MALDI ionization provided a better glycan profile than ESI but, at the same time, did not affect the ion mobility or fragmentation characteristics of the instrument. Also performing ionization by MALDI on the TWIMS-MS instrument led to much better fragmentation with higher resolution than could be obtained with a MALDI-TOF instrument.

Having established the advantages of MALDI profiling combined with full mass range fragmentation, the method

was used to obtain glycan profiles (Figure 2) and MS/MS data from the HIV glycoprotein gp120 (expressed in HEK 293T cells). Results are listed in Table 1 (columns 2 and 3).

Negative Ion

Because negative ion CID spectra of underivatized glycans provide more informative spectra than those recorded from positive ions, the ideal system would be a combination of MALDI ionization with CID fragmentation with the additional dimension of ion mobility for sample clean-up [58] and possible isomer separation. Earlier work [44] has shown that

Table 1. Masses and Compositions for the *N*-Glycans Found in the gp120 Samples

Compd. ^(a,b)	m/z ([M+Na] ⁺)		m/z ([M+NO ₃] ⁻)			m/z ([M-I] ⁻)		Composition			
	Found	Calc.	Found (Figure 5)	Found (Figure 6)	Calc.	Found	Calc.	Hex (Man, Gal)	GlcNAc	dHex (Fuc)	Neu5Ac
1	1257.4	1257.4	1296.4	1296.4	1296.4	1361.3	1361.3	5	2	0	0
2	1282.4	1282.4	-	-	1321.5	1386.4	1386.4	3	3	1	0
3	1298.4	1298.4	-	-	1337.4	1402.4	1402.4	4	3	0	0
4	1419.5	1419.5	1458.5	1458.5	1458.5	1523.4	1523.4	6	2	0	0
5	1444.5	1444.5	1483.5	1483.5	1483.5	1548.4	1548.4	4	3	1	0
6	1460.5	1460.5	1499.5	1499.5	1499.5	1564.4	1564.4	5	3	0	0
7	1485.5	1485.5	1524.5	1524.5	1524.5	1589.4	1589.4	3	4	1	0
8	1501.5	1501.5	-	-	1540.5	1605.4	1605.4	4	4	0	0
9	1581.5	1581.5	1620.5	1620.5	1620.5	1685.4	1685.4	7	2	0	0
10	1606.5	1606.6	1645.6	1645.6	1645.6	1710.5	1710.5	5	3	1	0
11	1622.5	1622.6	1661.6	1661.6	1661.6	1726.5	1726.5	6	3	0	0
12	1647.6	1647.6	1686.6	1686.6	1686.7	1751.5	1751.5	4	4	1	0
13	1663.6	1663.6	1702.6	-	1702.6	1767.5	1767.5	5	4	0	0
14	-	-	1727.6 ^(c)	1727.6 ^(c)	1727.6 ^(c)	1727.6 ^(c)	1727.6 ^(c)	5	3	0	1
15	1688.6	1688.6	1727.6	1727.6	1727.6	1792.5	1792.5	3	5	1	0
16	1743.6	1743.6	1782.6	1782.6	1782.6	1847.5	1847.5	8	2	0	0
17	1768.6	1768.6	1807.6	1807.6	1807.6	1872.5	1872.5	6	3	1	0
18	1793.6	1793.6	1832.7	-	1832.7	1897.6	1897.6	4	4	2	0
19	1809.6	1809.6	1848.7	1848.7	1848.7	1913.5	1913.6	5	4	1	0
20	-	-	1873.7 ^(c)	1873.7 ^(c)	1873.7 ^(c)	1873.6 ^(c)	1873.7 ^(c)	5	3	1	1
21	-	-	1889.7 ^(c)	1889.7 ^(c)	1889.7 ^(c)	1889.6 ^(c)	1889.7 ^(c)	6	3	0	1
22	1850.6	1850.6	1889.7	1889.6	1889.7	1954.7	1954.6	4	5	1	0
23	-	-	-	1914.7 ^(c)	1914.7 ^(c)	-	1914.7 ^(c)	4	4	1	1
24	-	-	1930.7 ^(c)	1930.7 ^(c)	1930.7 ^(c)	1930.7 ^(c)	1930.7 ^(c)	5	4	0	1
25	1891.7	1891.7	1930.7	1930.7	1930.7	1995.7	1995.6	3	6	1	0
26	1905.6	1905.6	1944.7	1944.7	1944.7	2009.5	2009.5	9	2	0	0
27	1955.7	1955.7	1994.7	-	1994.7	2059.7	2059.6	5	4	2	0
28	-	-	2035.7 ^(c)	2035.7 ^(c)	2035.7 ^(c)	2035.7 ^(c)	2035.7 ^(c)	6	3	1	1
29	2012.7	2012.7	2051.7	2051.7	2051.7	2116.6	2116.6	5	5	1	0
30	2028.7	2028.7	2067.7	-	2067.7	-	2132.6	6	5	0	0
31	2053.7	2053.7	2092.8	-	2092.7	2157.8	2157.7	4	6	1	0
32	-	-	2076.8 ^(c)	2076.8 ^(c)	2076.8 ^(c)	2076.7 ^(c)	2076.8 ^(c)	5	4	1	1
33	2122.7	2122.7	2161.7	2161.7	2161.7	2226.7	2226.6	5	4	1	1(Na)
34	-	-	2092.7 ^(c)	-	2092.8 ^(c)	-	2092.8 ^(c)	6	4	0	1
35	-	-	2117.7	-	2117.8	2117.7	2117.8	4	5	1	1
36	-	-	2133.7 ^(c)	-	2133.7 ^(c)	-	2133.7 ^(c)	5	5	0	1
37	2122.7	2122.7	2161.7	2161.9	2161.7	2226.6	2226.7	5	4	1	1(Na)
38	2174.8	2174.8	2213.8	-	2213.8	-	2278.7	6	5	1	0
39	2215.8	2215.8	2254.8	-	2254.8	-	2319.7	5	6	1	0
40	-	-	2295.8 ^(c)	-	2295.8 ^(c)	-	2295.8 ^(c)	6	5	0	1
41	2325.8	2325.8	-	-	2364.8	-	2429.7	5	5	1	1(Na)
42	2378.0	2377.8	-	-	2416.8	-	2481.8	6	6	1	0
43	-	-	-	2441.8 ^(c)	2441.9 ^(c)	-	2569.8 ^(c)	6	5	1	1
44	2488.0	2487.8	-	-	2526.8	-	2591.8	6	5	1	1(Na)
45	2540.0	2539.9	-	-	2578.9	-	2643.8	7	6	1	0

(a) Compounds as in Figures 2, 5, and 6

(b) Structures of the neutral glycans are shown in Scheme 1 (where determined)

(c) [M-H]⁻ ion

with MALDI-TOF systems using nitrogen lasers, good negative ion spectra could be obtained with THAP doped with a 1 M solution of ammonium nitrate. In the present work, several matrices (see Methods section) and the use of various ammonium salts were investigated to determine the optimum conditions for similar ion formation with the Synapt instrument which uses a Nd/Yag (355 nm) rather than a nitrogen laser (337 nm). Again, THAP proved to be the best matrix although HABA was nearly as good. Results with desialylated *N*-glycans from porcine thyroglobulin (mainly high-mannose and biantennary complex glycans) in the presence of various ammonium salts (0.5 μ L of a 1 M solution) are shown in the supplementary data (Figure S1). Results were essentially as found earlier with the MALDI-TOF instrument and are summarized in the Supplementary Data. The best adduct for producing a clean spectrum (virtually free from ions produced from minor impurities in the samples) proved to be nitrate. These adducts also produced excellent fragmentation spectra (transfer cell) of the same type as observed earlier following electrospray ionization. Sulfate and iodide, although producing strong spectra failed to yield fragment ions.

The MALDI-CID-MS (transfer cell) spectra were similar to those obtained by ESI (Figure 3 and additional spectra in Figure S2) and were more informative than those obtained

earlier using LIFT technology on a Bruker Ultraflex instrument (Bruker Daltonic, Bremen, Germany) or an ion trap-TOF instrument (Axima resonance) following MALDI ionization. Although the spectra from both of these instruments were of high quality, the abundance of low mass ions from the Bruker instrument was low and the low mass region of spectra recorded from the trap was missing. Low-mass ions are important for structural analysis of these compounds because they define the residues on the non-reducing termini. Spectra from the Synapt instruments displayed abundant fragment ions across the entire mass range with good resolution. The spectra of $\text{Man}_8\text{GlcNAc}_2$ shown in Figure 3 contain a prominent triplet of $^{2,4}\text{A}_6$, B_5 and $^{2,4}\text{A}_5$ ions defining the reducing terminus (the nomenclature introduced by Domon and Costello [63] is used to describe the fragment ions) formed by hydrogen abstraction from the OH group at position 3 of the GlcNAc residues. The masses of the $^{2,4}\text{A}$ ions can be used to show if fucose is present at C6 of the core GlcNAc residue. The ions labeled D, $[\text{D} - 18]^-$ and $^{0,3}\text{A}_4$, D and $[\text{D} - 18]^-$, define the composition of the 6-antenna and the D' ion defines the branching of this antenna. Further details of the negative ion fragmentation of these compounds are in references [29–32].

Sialylated glycans lost very little of their sialic acid; the profiles of glycans from bovine fetuin and porcine thyro-

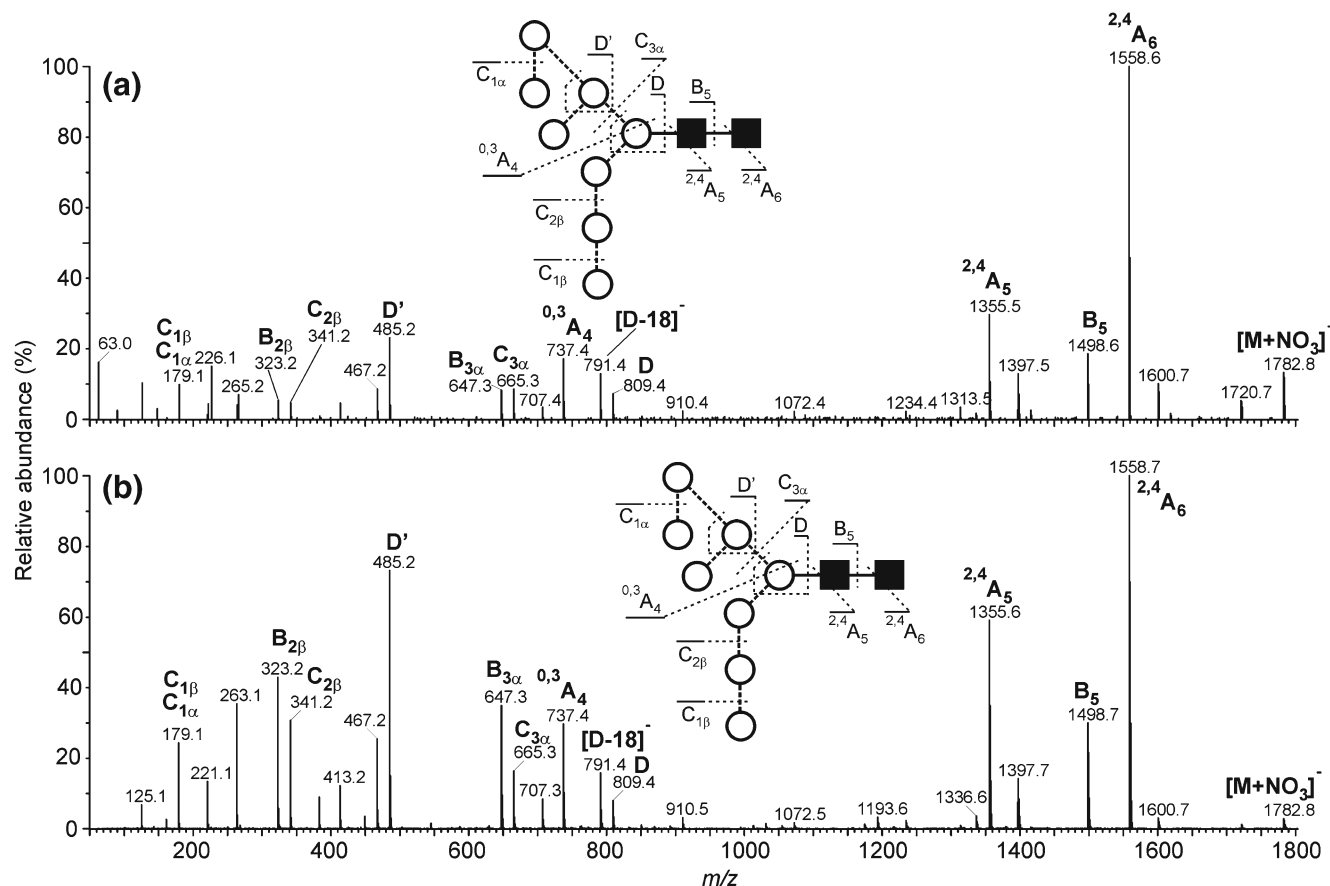


Figure 3. (a) Negative ion CID spectrum (transfer cell) of the nitrate adduct of high-mannose glycan $\text{Man}_8\text{GlcNAc}_2$ from gp120 recorded following ionization by MALDI and with a collision cell energy of 85 eV. (b) Fragmentation of the same compound ionized by electrospray (Q-TOF Ultima instrument, collision energy 70 eV)

globulin (Figure 4a) whose complex glycans are partially sialylated, contained prominent peaks produced by monosialylated compounds (the fetuin sample was rather old and had spontaneously lost sialic acid from the bi- and trisialylated glycans as determined by permethylation experiments). Also present in the spectra of the thyroglobulin glycans following removal of the sialic acids by acid hydrolysis were abundant ions produced from sulfated glycans similar to those reported by de Waard et al. [53] (Figure 4b). They were characterized by typical fragmentation spectra such as that shown in Figure 4c and showing

that such compounds were also relatively stable under these MALDI conditions. The major ion in the negative ion CID spectra of these compounds was at m/z 444 corresponding to $(\text{SO}_3)\text{Gal-GlcNAc}$ but, because the charge was localized on the sulfate group, the diagnostic, mainly cross-ring, ions that were present in the spectra of the neutral (adducted) glycans were missing. The spectra were dominated by B- and Y-type glycosidic fragments. Sialylated glycans showed similar spectra as the result of charge localization on the acid group but, not to the extent that all cross-ring fragments were absent. The spectra of monosialylated glycans, in particular,

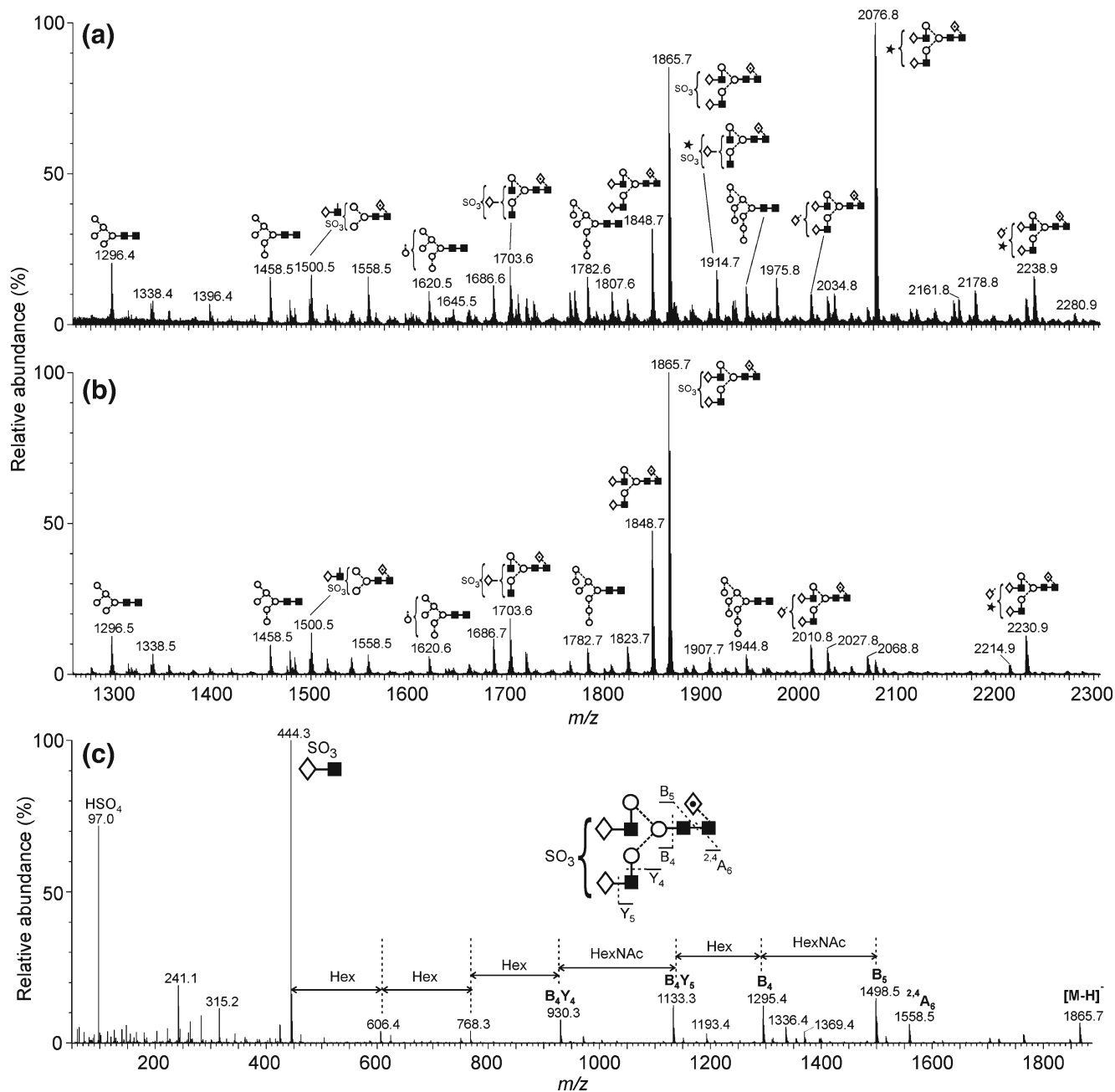


Figure 4. (a) Negative ion MALDI spectrum (nitrate adducts from THAP) of *N*-glycans released from porcine thyroglobulin. (b) Negative ion MALDI spectrum of *N*-glycans released from porcine thyroglobulin and desialylated with 1 % acetic acid. (c) Negative ion CID spectrum of the sulfated biantennary glycan $\text{Gal}_2\text{Man}_3\text{GlcNAc}_4\text{Fuc}_1$

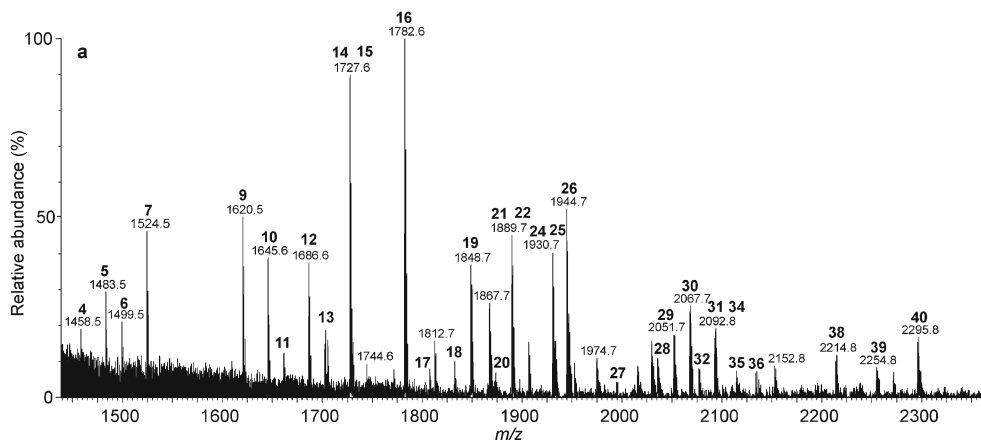


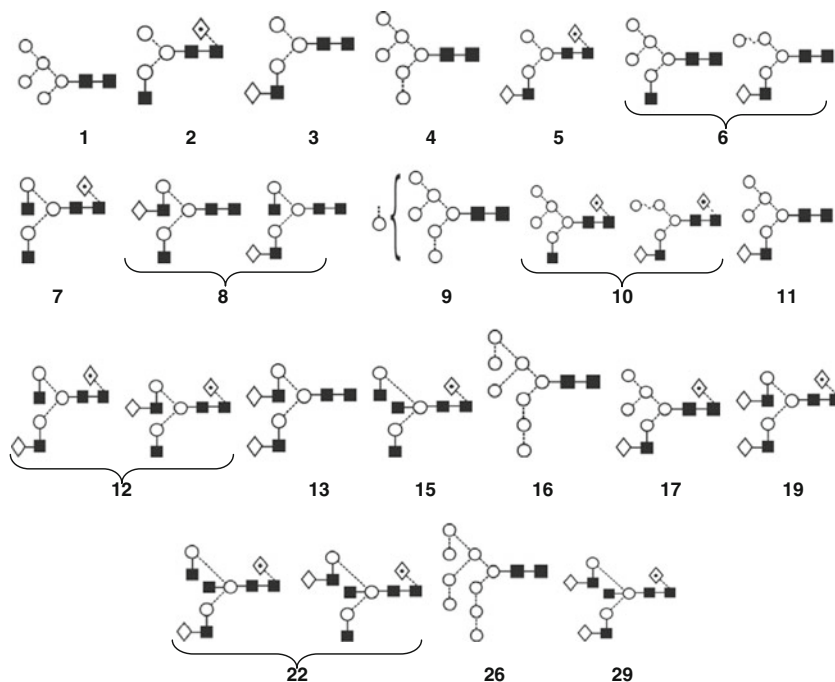
Figure 5. Negative ion MALDI spectrum (nitrate adducts from THAP) of *N*-glycans released in-gel from gp120 and cleaned with a Nafion membrane. Compounds, identified by the numbers on the peaks, are listed in Table 1 (column 4)

retain many of the diagnostic ions (data not shown but see reference [64]). However, these glycans can be neutralized by derivatization [33, 61], as mentioned above and, in some cases, the derivatization reaction can be exploited to provide linkage information for the sialic acids [34].

The method, using THAP doped with ammonium nitrate, was used to characterize *N*-glycans released from the recombinant HIV glycoproteins. Figure 5 shows the negative ion MALDI profile of glycans from gp120 with an N339A mutation expressed in HEK293 cells released with PNGase F from within an SDS-PAGE gel and cleaned with a Nafion 117 membrane [65]. A full list of the identified compounds is in Table 1 (columns 4 and 6), structures are in Scheme 1).

In some cases, sample amounts were so small that glycan ions were not visible in the MALDI spectra even after

extensive clean-up. In a previous paper [58], we reported that ion mobility could be used to extract the *N*-glycan ions from complex mixtures whose ESI spectra did not show evidence of the presence of such ions. Much of the non-carbohydrate material present in PNGase F-released glycans formed multiply charged ions that readily separated in the ion mobility cell. The same experiment with *N*-glycans released from gp120 in solution in the presence of NP-40 denaturant was repeated with MALDI ionization and the results are shown in Figure 6. No pre-mass spectrometric clean-up was employed in this experiment to see if ion mobility was able to visualize the glycan ions in such unpurified samples. No glycans were observed in the raw MALDI spectrum in negative ion mode (Figure 6a, nitrate adducts) but the glycan ions could be extracted (Figure 6d) from the Driftscope display (Figure 6b).



Scheme 1. Structures of the identified neutral glycans from gp120 (Figures 2, 5, and 6). Sialylated compounds are not listed

Their masses and deduced compositions are listed in Table 1 (columns 5 and 9–12). Structures have been determined earlier [58, 66–68] and those of the major neutral glycans are shown in Scheme 1 (the sialylated glycans are derivatives of these compounds and individual structures are not shown). Because MALDI produces mainly singly charged ions, separation of the glycan ions from the ions produced by background contamination was not as complete as that obtained with ESI but, nevertheless, most of the background was removed. Iodide was found, as described above, to produce stronger spectra than nitrate and, consequently, the sample was also examined as iodide adducts (Figure 6c); the spectrum is shown in Figure 6e and the glycans are listed in Table 1 (columns 7 and 8).

Although prominent ions were extracted by this technique, both spectra (nitrate and iodide adducts) contained additional ions that appeared to have been formed by further attachment of sodium nitrate and sodium iodide, respectively, to some of the glycans. Thus, the ion at m/z 2076 in the spectrum of the nitrate adducts (Figure 6d), which was produced by the sodium salt (37) of the monosialylated biantennary glycan, was accompanied by additional ions at m/z 2161 and 2246 corresponding to complexes with one and two equivalents of NaNO_3 . In the spectrum of the iodide adducts (Figure 6e) corresponding NaI adduct ions were present at m/z 2377 and 2526. Similar adducts of other compounds produced the rather complex spectra. The

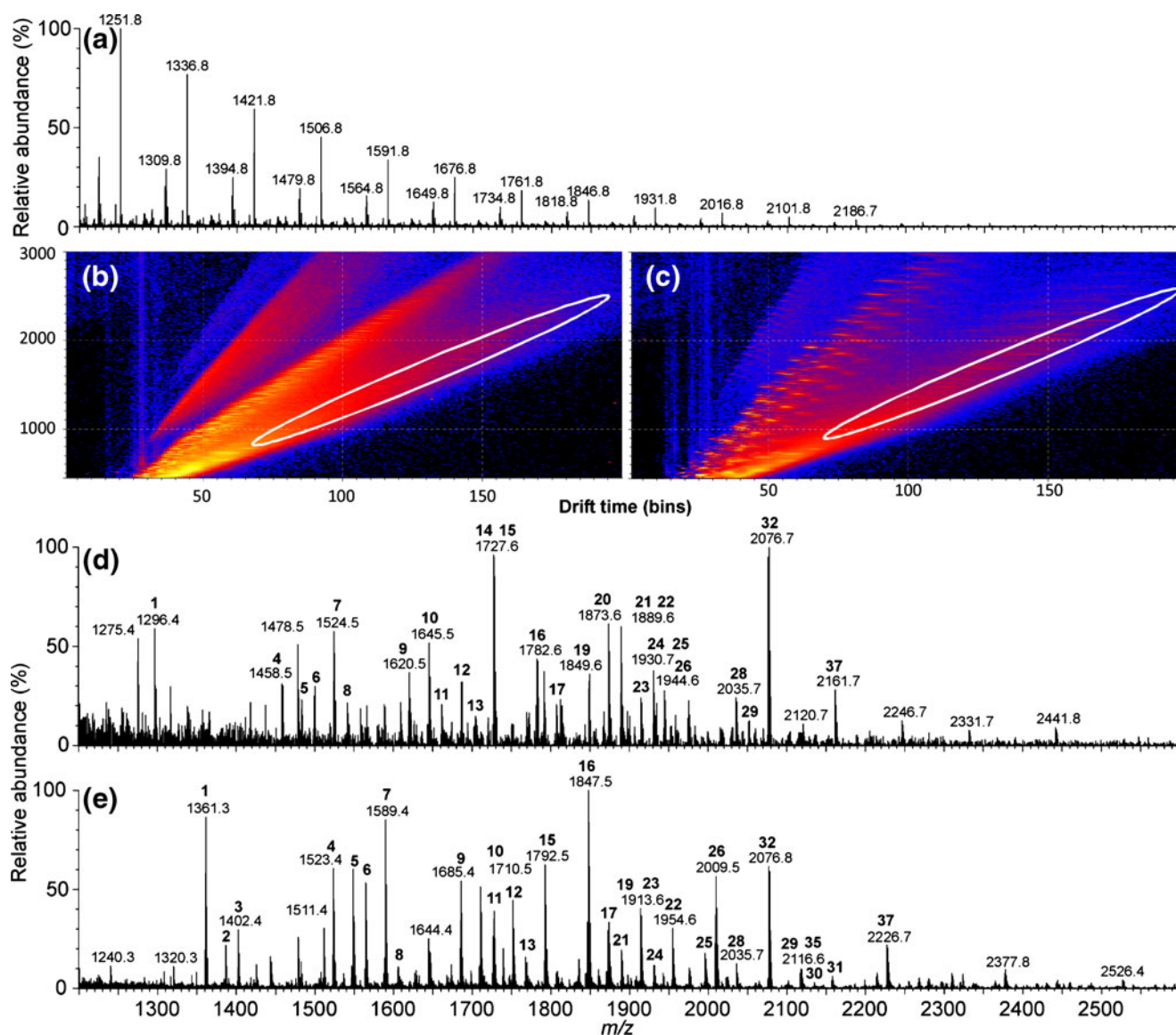


Figure 6. (a) Negative ion MALDI spectrum of gp120 glycans released in solution in the presence of NP40 denaturant, ionized by MALDI from THAP doped with ammonium nitrate (no mobility clean-up). (b) DriftScope display of gp120 glycans released in solution in the presence of NP40 denaturant and ionized by MALDI from THAP doped with ammonium nitrate. The region of the DriftScope display corresponding to glycan ions is indicated by the white oval. (c) The same sample but acquired as iodide adducts. (d) Negative ion mobility-extracted spectrum of gp120 glycans released in solution and extracted by ion mobility [circled area on (b)]. (e) The same glycans analysed as iodide adducts

sodium in these adducts presumably originated from the original sample but could be removed with suitable clean-up procedures, such as the use of a Nafion membrane [65], our current preferred technique. These adducts showed a different drift-time-*m/z* profile to the main glycans and could, thus be partially removed using the DriftScope display. Also present in the negative ion spectra were $[M - H]^-$ ions formed from the free sialylated glycans.

Separation of Isobaric Glycans by Ion Mobility

By use of ion mobility it has been possible to separate small isomeric *N*-glycans on account of their different drift times [62, 69]. Several of the glycans from gp120 are isobaric and/or isomeric; consequently the glycans whose spectra are shown in Figures 2 (positive ion) and 5 (negative ion) were examined to see if any of these compounds could be separated. Two glycans showing clear separation were those of composition Hex₅GlcNAc₃Fuc₁ (*m/z* 1606, positive ion and 1645, negative ion). The ATD profile and two CID spectra of the constituent glycans are shown in Figure 2b, c, and d, respectively. Similar results were obtained for the negative ions (data not shown). Some other ATD peaks showed peak broadening suggesting additional separations; discussion of these separations will form part of a further communication.

Conclusions

The combination of negative ion MALDI profiling followed by CID provides a very powerful combination for *N*-glycan analysis, particularly when combined with ion mobility for sample clean-up and possible isomer detection. MALDI is preferred to ESI for glycan profiling because of its ability to produce predominantly singly charged ions which, for neutral glycans at least, reflect the quantitative composition of the mixture. ESI spectra can suffer from multiple charging which, although a bonus for large molecules, causes problems with glycan analysis because of preferential formation of doubly and sometimes triply charged ions from the larger glycans; this effect distorts the glycan profile. In addition, ESI spectra of glycans usually contain fragment ions that also distort the profile. For negative ion formation from neutral glycans in this work, the strongest signals were obtained by use of iodide and sulfate offering the possibility of high sensitivity detection for trace analysis. Unfortunately these adducts did not produce fragment ions, but excellent fragmentation was obtained from the other adducts with nitrate being particularly useful. Fragmentation of negative ions from anion-adducted carbohydrates provided considerably more structural information than fragmentation of positive ions because of the formation of specific cross-ring fragments. Thus, there was less ambiguity in the spectra; ambiguity is caused predominantly by equivalent glycosidic cleavages from the several antennae present in these compounds. Specific structural features that can be acquired

included detailed information on the location of fucose residues, determination of specific isomers of tri-antennary glycans, and an indication of the presence of “bisecting” GlcNAc residues. Most of these properties are difficult to detect by more traditional methods.

Furthermore, the combination of MALDI with ion mobility allowed the latter function to be used to strip out contaminating ions allowing glycan ions to be recovered from spectra that showed little or no sign of them without mobility extraction. Thus, MALDI, followed by ion mobility and CID fragmentation can be used to examine the products of enzymatic glycan release without additional clean-up, allowing for rapid analysis, and can also be used to great advantage with samples containing very little glycan material, such as the analysis of HIV glycans from infectious virions [70, 71].

In conclusion, the combination of MALDI ionization, negative ion fragmentation, and ion mobility for clean-up of both the glycan profile and fragmentation spectra provides a very powerful system for *N*-glycan analysis that requires no derivatization step and the minimum of sample clean-up.

Acknowledgments

The authors thank Professor Raymond Dwek for his help and encouragement. They also thank the Biotechnology and Biological Sciences Research Council for funds to purchase the ToFSpec 2E mass spectrometer. Financial support was also provided by the Oxford Glycobiology bequest and the International AIDS Vaccine Initiative. Thanks are also due to Rad Kozak of Ludger Ltd. (Abingdon UK) for performing the permethylation experiments.

References

- Varki, A., Cummings, R.D., Esko, J.D., Freeze, H.H., Stanley, P., Bertozzi, C.R., Hart, G.W., Etzler, M.E.: *Essentials of Glycobiology*, 2nd edn. Cold Spring Harbor Laboratory Press (2008)
- Dwek, R.A., Edge, C.J., Harvey, D.J., Wormald, M.R., Parekh, R.B.: Analysis of glycoprotein-associated oligosaccharides. *Ann. Rev. Biochem.* **62**, 65–100 (1993)
- Harvey, D.J.: Matrix-assisted laser desorption/ionization mass spectrometry of carbohydrates. *Mass Spectrom. Rev.* **18**, 349–451 (1999)
- Zaia, J.: Mass spectrometry of oligosaccharides. *Mass Spectrom. Rev.* **23**, 161–227 (2004)
- Harvey, D.J.: Proteomic analysis of glycosylation: Structural determination of *N*- and *O*-linked glycans by mass spectrometry. *Expert Rev. Proteom.* **2**, 87–101 (2005)
- Harvey, D.J.: Structural determination of *N*-linked glycans by matrix-assisted laser desorption/ionization and electrospray ionization mass spectrometry. *Proteomics* **5**, 1774–1786 (2005)
- Geyer, H., Geyer, R.: Strategies for analysis of glycoprotein glycosylation. *Biochim. Biophys. Acta* **1764**, 1853–1869 (2006)
- Medzihradzky, K.F.: Characterization of protein *N*-glycosylation. *Methods Enzymol.* **405**, 116–138 (2005)
- Morelle, W., Faid, V., Chirat, F., Michalski, J.C.: Analysis of *N*- and *O*-linked glycans from glycoproteins using MALDI-TOF mass spectrometry. *Methods Molec. Biol.* **534**, 5–21 (2009)
- Mariño, K., Bones, J., Kattla, J.J., Rudd, P.M.: A systematic approach to protein glycosylation analysis: A path through the maze. *Nat. Chem. Biol.* **6**, 713–723 (2010)
- Morelle, W.: Analysis of glycosylation and other post-translational modifications by mass spectrometry. *Curr. Anal. Chem.* **5**, 144–165 (2009)

12. Pabst, M., Altmann, F.: Glycan analysis by modern instrumental methods. *Proteomics* **11**, 631–643 (2011)
13. Yamada, K., Kakehi, K.: Recent advances in the analysis of carbohydrates for biomedical use. *J. Pharm. Biomed. Anal.* **55**, 702–727 (2011)
14. Angel, A.S., Nilsson, B.: Analysis of glycoprotein oligosaccharides by fast atom bombardment mass spectrometry. *Biomed. Environ. Mass Spectrom.* **19**, 721–730 (1990)
15. Dell, A., Thomas-Oates, J.E.: Fast atom bombardment-mass spectrometry (FAB-MS): Sample preparation and analytical strategies. In: Biermann, C.J., McGinnis, G.D. (eds.) *Analysis of Carbohydrates by GLC and MS*, pp. 217–235. CRC Press, Boca Raton (1989)
16. Dell, A., Carman, N.H., Tiller, P.R., Thomas-Oates, J.E.: Fast atom bombardment mass spectrometric strategies for characterizing carbohydrate-containing biopolymers. *Biomed. Environ. Mass Spectrom.* **16**, 19–24 (1988)
17. Mawhinney, T.P., Chance, D.L.: Structural elucidation by fast atom bombardment mass spectrometry of multisulfated oligosaccharides isolated from human respiratory mucous glycoproteins. *J. Carbohydr. Chem.* **13**, 825–840 (1994)
18. Dell, A., Carman, N.H., Tiller, P.R., Thomas-Oates, J.E.: Fast atom bombardment mass spectrometric strategies for characterising carbohydrate-containing biopolymers. *Biomed. Environ. Mass Spectrom.* **16**, 19–24 (1987)
19. Harvey, D.J.: Analysis of carbohydrates and glycoconjugates by matrix-assisted laser desorption/ionization mass spectrometry: An update for the period 2005–2006. *Mass Spectrom. Rev.* **30**, 1–100 (2011)
20. Harvey, D.J.: Carbohydrate analysis by ESI and MALDI. In: Cole, R.B. (ed.) *Electrospray and MALDI Mass Spectrometry: Fundamentals, Instrumentation, Practicalities, and Biological Applications*, 2nd edn, pp. 723–769. John Wiley and Sons Inc, Hoboken (2010)
21. Reinhold, V.N., Reinhold, B.B., Costello, C.E.: Carbohydrate molecular weight profiling, sequence, linkage, and branching data: ES-MS and CID. *Anal. Chem.* **67**, 1772–1784 (1995)
22. Harvey, D.J., Bateman, R.H., Green, M.R.: High-energy collision-induced fragmentation of complex oligosaccharides ionized by matrix-assisted laser desorption/ionization mass spectrometry. *J. Mass Spectrom.* **32**, 167–187 (1997)
23. Mechref, Y., Novotny, M.V., Krishnan, C.: Structural characterization of oligosaccharides using MALDI-TOF/TOF tandem mass spectrometry. *Anal. Chem.* **75**, 4895–4903 (2003)
24. Stephens, E., Maslen, S.L., Green, L.G., Williams, D.H.: Fragmentation characteristics of neutral *N*-linked glycans using a MALDI-TOF/TOF tandem mass spectrometer. *Anal. Chem.* **76**, 2343–2354 (2004)
25. Harvey, D.J., Martin, R.L., Jackson, K.A., Sutton, C.W.: Fragmentation of *N*-linked glycans with a MALDI-ion trap time-of-flight mass spectrometer. *Rapid Commun. Mass Spectrom.* **18**, 2997–3007 (2004)
26. Ashline, D., Singh, S., Hanneman, A., Reinhold, V.: Congruent strategies for carbohydrate sequencing. I. Mining structural details by MSⁿ. *Anal. Chem.* **77**, 6250–6262 (2005)
27. Zhang, H., Singh, S., Reinhold, V.N.: Congruent strategies for carbohydrate sequencing. 2. FragLib: An MSⁿ spectral library. *Anal. Chem.* **77**, 6263–6270 (2005)
28. Jiao, J., Zhang, H., Reinhold, V.N.: High performance IT-MSⁿ sequencing of glycans (spatial resolution of ovalbumin isomers). *Int. J. Mass Spectrom.* **303**, 109–117 (2011)
29. Harvey, D.J.: Fragmentation of negative ions from carbohydrates. Part 2. Fragmentation of high-mannose *N*-linked glycans. *J. Am. Soc. Mass Spectrom.* **16**, 631–646 (2005)
30. Harvey, D.J.: Fragmentation of negative ions from carbohydrates. Part 1. Use of nitrate and other anionic adducts for the production of negative ion electrospray spectra from *N*-linked carbohydrates. *J. Am. Soc. Mass Spectrom.* **16**, 622–630 (2005)
31. Harvey, D.J.: Fragmentation of negative ions from carbohydrates: Part 3. Fragmentation of hybrid and complex *N*-linked glycans. *J. Am. Soc. Mass Spectrom.* **16**, 647–659 (2005)
32. Harvey, D.J., Royle, L., Radcliffe, C.M., Rudd, P.M., Dwek, R.A.: Structural and quantitative analysis of *N*-linked glycans by MALDI and negative ion nanospray mass spectrometry. *Anal. Biochem.* **376**, 44–60 (2008)
33. Powell, A.K., Harvey, D.J.: Stabilization of sialic acids in *N*-linked oligosaccharides and gangliosides for analysis by positive ion matrix-assisted laser desorption-ionization mass spectrometry. *Rapid Commun. Mass Spectrom.* **10**, 1027–1032 (1996)
34. Wheeler, S.F., Domann, P., Harvey, D.J.: Derivatization of sialic acids for stabilization in matrix-assisted laser desorption/ionization mass spectrometry and concomitant differentiation of $\alpha(2-3)$ and $\alpha(2-6)$ isomers. *Rapid Commun. Mass Spectrom.* **23**, 303–312 (2009)
35. Sekiya, S., Wada, Y., Tanaka, K.: Derivatization for stabilizing sialic acids in MALDI-MS. *Anal. Chem.* **77**, 4962–4968 (2005)
36. Nonami, H., Tanaka, K., Fukuyama, Y., Erra-Balsells, R.: β -Carboline alkaloids as matrices for UV-Matrix-assisted laser desorption/ionization time-of-flight mass spectrometry in positive and negative ion modes. Analysis of proteins of high molecular mass, and of cyclic and acyclic oligosaccharides. *Rapid Commun. Mass Spectrom.* **12**, 285–296 (1998)
37. Becher, J., Muck, A., Mithöfer, A., Svatoš, A., Boland, W.: Negative ion mode matrix-assisted laser desorption/ionization time-of-flight mass spectrometric analysis of oligosaccharides using halide adducts and 9-aminoacridine matrix. *Rapid Commun. Mass Spectrom.* **22**, 1153–1158 (2008)
38. Cai, Y., Jiang, Y., Cole, R.B.: Anionic adducts of oligosaccharides by matrix-assisted laser desorption/ionization time-of-flight mass spectrometry. *Anal. Chem.* **75**, 1638–1644 (2003)
39. Suzuki, H., Yamagaki, T., Tachibana, K.: Optimization of matrix and amount of ammonium chloride additive for effective ionization of neutral oligosaccharides as chloride ion adducts in negative-mode MALDI-TOF mass spectrometry. *J. Mass Spectrom. Soc. Jpn.* **53**, 227–229 (2005)
40. Suzuki, H., Yamagaki, T., Tachibana, K.: Optimization for effective ionization of neutral oligosaccharides in negative-ion MALDI-MS. *Nippon Kagakukai Koen Yokoshu* **86**, 503 (2006)
41. Wong, A.W., Cancilla, M.T., Voss, L.R., Lebrilla, C.B.: Anion dopant for oligosaccharides in matrix-assisted laser desorption/ionization mass spectrometry. *Anal. Chem.* **71**, 205–211 (1999)
42. Wong, A.W., Wang, H., Lebrilla, C.B.: Selection of anionic dopant for quantifying desialylation reactions with MALDI-FTMS. *Anal. Chem.* **72**, 1419–1425 (2000)
43. Yamagaki, T., Suzuki, H., Tachibana, K.: Solid-phase fluorescence and ionization efficiency in negative-ion matrix-assisted laser desorption/ionization of neutral oligosaccharides: Interaction between β -carboline matrix and ammonium salt. *J. Am. Soc. Mass Spectrom.* **18**, 714–723 (2007)
44. Domann, P., Spencer, D.I.R., Harvey, D.J.: Production and fragmentation of negative ions from neutral *N*-linked carbohydrates ionized by matrix-assisted laser desorption/ionization. *Rapid Commun. Mass Spectrom.* **26**, 469–479 (2012)
45. Suzuki, H., Yamagaki, T., Tachibana, K.: Study of negative-ion matrix-assisted laser desorption/ionization mass spectrometry of neutral oligosaccharides II: Efficient negative ionization of neutral carbohydrates with interaction between matrix and salt. *J. Mass Spectrom. Soc. Japan* **55**, 137–144 (2007)
46. Yamagaki, T., Nakanishi, H.: Negative-mode matrix-assisted laser desorption/ionization mass spectrometry of maltoheptaose and cyclomalto-oligosaccharides. *J. Mass Spectrom. Soc. Japan* **50**, 204–207 (2002)
47. Yamagaki, T., Suzuki, H., Tachibana, K.: In-source and post-source decay in negative-ion matrix-assisted laser desorption/ionization time-of-flight mass spectrometry of neutral oligosaccharides. *Anal. Chem.* **77**, 1701–1707 (2005)
48. Yamagaki, T., Suzuki, H., Tachibana, K.: A comparative study of the fragmentation of neutral lacto-oligosaccharides in negative-ion mode by UV-MALDI-TOF and UV-MALDI ion-trap/TOF mass spectrometry. *J. Am. Soc. Mass Spectrom.* **17**, 67–74 (2006)
49. Yamagaki, T., Suzuki, H., Tachibana, K.: Semiquantitative analysis of isomeric oligosaccharides by negative-ion mode UV-MALDI TOF post-source decay mass spectrometry and their fragmentation mechanism study at *N*-acetyl hexosamine moiety. *J. Mass Spectrom.* **41**, 454–462 (2006)
50. Patel, T., Bruce, J., Merry, A., Bigge, C., Wormald, M., Jaques, A., Parekh, R.: Use of hydrazine to release in intact and unreduced form both *N*- and *O*-linked oligosaccharides from glycoproteins. *Biochemistry* **32**, 679–693 (1993)
51. Wing, D.R., Field, M.C., Schmitz, B., Thor, G., Dwek, R.A., Schachner, M.S., Rademacher, T.W.: The use of large-scale hydrazinolysis in the preparation of *N*-linked oligosaccharide libraries: Application to brain tissue. *Glycoconj. J.* **9**, 293–301 (1992)
52. Fu, D., Chen, L., O'Neill, R.A.: A detailed structural characterization of ribonuclease B oligosaccharides by ¹H NMR spectroscopy and mass spectrometry. *Carbohydr. Res.* **261**, 173–186 (1994)
53. de Waard, P., Koorevaar, A., Kamerling, J.P., Vliegthart, J.F.G.: Structure determination by ¹H NMR spectroscopy of (sulfated)

- sialylated *N*-linked carbohydrate chains released from porcine thyroglobulin by peptide-*N*^l-(*N*-acetyl- β -glucosaminyl)asparagine amidase-F. *J. Biol. Chem.* **266**, 4237–4243 (1991)
54. Kamerling, J.P., Rijkse, I., Maas, A.A.M., van Kuik, J.A., Vliegthart, J.F.G.: Sulfated *N*-linked carbohydrate chains in porcine thyroglobulin. *FEBS Letts.* **241**, 246–250 (1988)
 55. Da Silva, M.L.C., Stubbs, H.J., Tamura, T., Rice, K.G.: ¹H-NMR characterization of a hen ovalbumin tyrosinamide *N*-linked oligosaccharide library. *Arch. Biochem. Biophys.* **318**, 465–475 (1995)
 56. Harvey, D.J., Wing, D.R., Küster, B., Wilson, I.B.H.: Composition of *N*-linked carbohydrates from ovalbumin and co-purified glycoproteins. *J. Am. Soc. Mass Spectrom.* **11**, 564–571 (2000)
 57. Green, E.D., Adelt, G., Baenziger, J.U., Wilson, S., van Halbeek, H.: The asparagine-linked oligosaccharides on bovine fetuin. Structural analysis of *N*-glycanase-released oligosaccharides by 500-Megahertz ¹H-NMR spectroscopy. *J. Biol. Chem.* **263**, 18253–18268 (1988)
 58. Harvey, D.J., Sobott, F., Crispin, M., Wrobel, A., Bonomelli, C., Vasiljevic, S., Scanlan, C.N., Scarff, C., Thalassinos, K., Scrivens, J.H.: Ion mobility mass spectrometry for extracting spectra of *N*-glycans directly from incubation mixtures following glycan release: Application to glycans from engineered glycoforms of intact, folded HIV gp120. *J. Am. Soc. Mass Spectrom.* **22**, 568–581 (2011)
 59. Dunlop, D.C., Bonomelli, C., Mansab, F., Vasiljevic, S., Doores, K.J., Wormald, M.R., Palma, A.S., Feizi, T., Harvey, D.J., Dwek, R.A., Crispin, M., Scanlan, C.N.: Polysaccharide mimicry of the epitope of the broadly neutralizing anti-HIV antibody, 2G12, induces enhanced antibody responses to self oligomannose glycans. *Glycobiology* **20**, 812–823 (2010)
 60. Giles, K., Pringle, S.D., Worthington, K.R., Little, D., Wildgoose, J.L., Bateman, R.H.: Applications of a travelling wave-based radio-frequency-only stacked ring ion guide. *Rapid Commun. Mass Spectrom.* **18**, 2401–2414 (2004)
 61. Hansson, G.C., Bouhours, J.-F., Karlsson, H., Carlstedt, I.: Analysis of sialic acid-containing mucin oligosaccharides from porcine small intestine by high-temperature gas chromatography-mass spectrometry of their dimethylamides. *Carbohydr. Res.* **221**, 179–189 (1991)
 62. Williams, J.P., Grabenauer, M., Carpenter, C.J., Holland, R.J., Wormald, M.R., Giles, K., Harvey, D.J., Bateman, R.H., Scrivens, J.H., Bowers, M.T.: Characterization of simple isomeric oligosaccharides and the rapid separation of glycan mixtures by ion mobility mass spectrometry. *Int. J. Mass Spectrom.* **298**, 119–127 (2010)
 63. Domon, B., Costello, C.E.: A systematic nomenclature for carbohydrate fragmentations in FAB-MS/MS spectra of glycoconjugates. *Glycoconj. J.* **5**, 397–409 (1988)
 64. Harvey, D.J., Rudd, P.M.: Fragmentation of negative ions from *N*-linked carbohydrates. Part 5: Anionic *N*-linked glycans. *Int. J. Mass Spectrom.* **305**, 120–130 (2011)
 65. Börnsen, K.O., Mohr, M.D., Widmer, H.M.: Ion exchange and purification of carbohydrates on a Nafion(R) membrane as a new sample pretreatment for matrix-assisted laser desorption-ionization mass spectrometry. *Rapid Commun. Mass Spectrom.* **9**, 1031–1034 (1995)
 66. Zhu, X., Borchers, C., Bienstock, R.J., Tomer, K.B.: Mass spectrometric characterization of the glycosylation pattern of HIV-gp120 expressed in CHO cells. *Biochemistry* **39**, 11194–11204 (2000)
 67. Cutalo, J.M., Deterding, L.J., Tomer, K.B.: Characterization of glycopeptides from HIV-1_{SF2} gp120 by liquid chromatography mass spectrometry. *J. Am. Soc. Mass Spectrom.* **15**, 1545–1555 (2004)
 68. Go, E.P., Irungu, J., Zhang, Y., Dalpathado, D.S., Liao, H.-X., Sutherland, L.L., Alam, S.M., Haynes, B.F., Desaire, H.: Glycosylation site-specific analysis of HIV envelope proteins (JR-FL and CON-S) reveals major differences in glycosylation site occupancy, glycoform profiles, and antigenic epitopes' accessibility. *J. Proteome Res.* **7**, 1660–1674 (2008)
 69. Plasencia, M.D., Isailovic, D., Merenbloom, S.I., Mechref, Y., Clemmer, D.E.: Resolving and assigning *N*-linked glycan structural isomers from ovalbumin by IMS-MS. *J. Am. Soc. Mass Spectrom.* **19**, 1706–1715 (2008)
 70. Bonomelli, C., Doores, K.J., Dunlop, D.C., Thaney, V., Dwek, R.A., Burton, D.R., Crispin, M., Scanlan, C.N.: The glycan shield of HIV is predominantly oligomannose independently of production system or viral clade. *PLoS One* **6**, e23521 (2011)
 71. Doores, K.J., Bonomelli, C., Harvey, D.J., Vasiljevic, S., Dwek, R.A., Burton, D.R., Crispin, M., Scanlan, C.N.: Envelope glycans of immunodeficiency virions are almost entirely oligomannose antigens. *Proc. Natl. Acad. Sci. U. S. A.* **107**, 13800–13805 (2010)
 72. Harvey, D.J., Merry, A.H., Royle, L., Campbell, M.P., Dwek, R.A., Rudd, P.M.: Proposal for a standard system for drawing structural diagrams of *N*- and *O*-linked carbohydrates and related compounds. *Proteomics* **9**, 3796–3801 (2009)